From Viewpoint of Reserve Provider: A Day-ahead Multi-stage Robust Optimization Reserve Provision Method for Microgrid with Energy Storage

Ye Tang, *Graduate Student Member*, *IEEE*, Qiaozhu Zhai, *Member*, *IEEE*, and Yuzhou Zhou, *Member*, *IEEE*

***Abstract*—Energy storage (ES), as a fast response technology, creates an opportunity for microgrid (MG) to participate in the reserve market such that MG with ES can act as an independent reserve provider. However, the potential value of MG with ES in the reserve market has not been well realized. From the viewpoint of reserve provider, a novel day-ahead model is proposed comprehensively considering the effect of the real-time scheduling process, which differs from the model that MG with ES acts as a reserve consumer in most existing studies. Based on the proposed model, MG with ES can schedule its internal resources to give reserve service to other external systems as well as to realize optimal self-scheduling. Considering that the proposed model is just in concept and cannot be directly solved, a multi-stage robust optimization reserve provision method is proposed, which leverages the structure of model constraints. Next, the original model can be converted into a mixed-integer linear programming problem and the model is tractable with guaranteed solution feasibility. Numerical tests in a real-world context are provided to demonstrate efficient operation and economic performance.**

***Index Terms*—Reserve service, energy storage, microgrid, optimal self-scheduling, multi-stage robust optimization.**

NOMENCLATURE

A. Indices and Sets

Ω	Uncertainty set
Ω_t	Conditional uncertainty set
R	Real set
t	Index of time period
$[1:T]$	Set of time periods

B. Parameters

τ	Length of each time period
λ^+, λ^-	Prices for purchasing electricity from main grid and selling electricity to main grid
μ^+, μ^-	Day-ahead up-reserve and down-reserve prices
η_d, η_c	Discharging and charging efficiencies of energy storage (ES)
$\bar{d}, \underline{d}$	Bounds of load demands
E_0	Initial ES level
$\bar{E}, \underline{E}$	Bounds of ES level
$\bar{g}, \underline{g}$	Bounds of power exchange limits, i. e., allowable range of power exchange between microgrid (MG) and main grid
$\bar{P}^{\mathrm{dis}}, \bar{P}^{\mathrm{ch}}$	The maximum discharging and charging power of ES
$\bar{p}^{\mathrm{PV}}, \underline{p}^{\mathrm{PV}}$	Bounds of photovoltaic power outputs
$\bar{w}, \underline{w}$	Bounds of wind power outputs

C. Uncertain Variables

d	Uncertain load demand
p^{PV}	Photovoltaic output
r^+	Uncertain up-reserve demand
r^-	Uncertain down-reserve demand
w	Wind power output

D. Unfolded (Realized) Uncertain Variables up to Time Period t

$\boldsymbol{\xi}_{[t]}$	Realized uncertainty vector
$\boldsymbol{d}_{[t]}$	Realized load demand vector
$\boldsymbol{p}^{\mathrm{PV}}_{[t]}$	Realized photovoltaic power output vector
$\boldsymbol{r}^+_{[t]}$	Realized up-reserve demand vector
$\boldsymbol{r}^-_{[t]}$	Realized down-reserve demand vector
$\boldsymbol{w}_{[t]}$	Realized wind power output vector

Manuscript received: September 28, 2023; revised: January 9, 2024; accepted: March 6, 2024. Date of CrossCheck: March 6, 2024. Date of online publication: May 3, 2024.

This work was supported in part by National Key Research and Development Program of China (No. 2022YFA1004600), China Postdoctoral Science Foundation (No. 2022M722533), and National Natural Science Foundation of China (No. 11991023).

Y. Tang, Q. Zhai (corresponding author), and Y. Zhou are with Systems Engineering Institute, MOEKLINNS Lab, Xi'an Jiaotong University, Xi'an 710049, China (e-mail: yetang@stu.xjtu.edu.cn; qzzhai@sei.xjtu.edu.cn; yzzhou@sei.xjtu.edu.cn).

DOI: 10.35833/MPCE.2023.000718

E. Decision Variables

$\tilde{d}_t$ Day-ahead power injection of MG from (positive value)/to (negative value) the main grid determined in the day-ahead stage, which is a curve rather than a region in real-time stage

E_t ES level

$\bar{E}_t^{\text{true}}$, $\underline{E}_t^{\text{true}}$ Safe and feasible bounds of ES level, which are decision variables different from $\bar{E}$, $\underline{E}$

P_t^{sto} Charging (negative value) or discharging (positive value) power of ES

p_t^{PVcur} Curtailment of photovoltaic power outputs

R_t^+ Up-reserve capacity limit

R_t^- Down-reserve capacity limit

w_t^{cur} Curtailment of wind power outputs

x Real-time decision variables

y Day-ahead decision variables

F. Functions

$h(\cdot)$ Auxiliary function

$h^{-1}(\cdot)$ Inverse function of $h(\cdot)$

I. Introduction

THE rapid development of renewable energy sources (RESs) has stimulated the evolution of the electric energy sector [1], [2]. To be specific, the traditional thermal units are gradually replaced by RESs to confront the environmental pollution and energy crisis [3]. Nevertheless, RESs, especially wind and solar energy, cannot provide a constant power supply due to the high intermittent, strong fluctuation, poor controllability, and lower forecasting accuracy [4], [5]. Therefore, the continuous increase in the penetration rate of RESs may pose a significant challenge to the secure, stable, and economic operation and scheduling of energy systems.

Microgrid (MG) is a small-scale power system characterized by high reliability and strong flexibility, which can provide localized power supply, demand-side management, and energy trading functions. MG is a promising way to integrate RESs and provides a viable solution to improving power system flexibility and long-term development [6]-[8]. A typical MG consists of multiple distributed generations, energy storage (ES), and consumption devices. ES is the major physical component for mitigating potential RES fluctuations, dealing with tricky demand-supply imbalance issues, and reducing the electricity cost [9]-[11].

The economic scheduling of MG integrated with ES and uncertainty, as a typical and critical content, aims to minimize operation costs while satisfying device or contractual constraints [12]. The main difficulty in such a scheduling problem arises from the state of charge (SOC) character of ES under uncertainty, e.g., uncertain renewable energy injection and uncertain load demand. In other words, feasible and economic solutions should satisfy the nonlinear coupling constraints (SOC character) under any realization of the uncertain renewables during each time period. Therefore, two mainstream methods, including stochastic optimization (SO) method [13]-[15] and robust optimization (RO) method [16]-[22], have been proposed to realize the optimal scheduling of MG with uncertainty injection and ES.

In SO method, uncertainty is modeled by the scenarios under suitable discrete [23]. The reliability and economy of the scheduling solution need to be verified in each scenario. In contrast, uncertainty in RO method is expressed as uncertainty sets [24]. As a representative of RO method, the two-stage RO method can achieve optimal scheduling [16]-[18] based on uncertainty sets, with the "min-max" structure to ensure the worst-case feasibility. However, some recent works have reached a consensus that the scheduling solutions provided by SO method and two-stage RO method may be infeasible in real-time operation [25]-[28]. In recognizing this issue, multi-stage RO methods are considered to be the most efficient [19]-[22], with one way based on the the affine function assumption, while the other establishing auxiliary constraints based on the specific formulation structure [29].

Regarding [13]-[22], the main grid plays an important role in compensating for possible power generation fluctuations (aroused by the integrated RES as well as power consumption uncertainty from load demand) by providing sufficient reserve service for MG. In this way, MG with ES is regarded as a reserve consumer. However, it is not an economical and reliable solution since the reserve burden of the main grid and the difficulty for the main grid in scheduling will increase, and the reserve potential of MG with ES is not fully utilized.

Recognizing the potential of ES in providing reserve, we consider MG with ES as a reserve provider in this paper. It means that MG with ES will not only achieve optimal self-scheduling without the reserve support from the main grid, but also provide reserve service to the main grid in the face of uncertainty, particularly uncertain reserve demands. Existing research works on ES reserve provision are primarily established from the viewpoint of independent system operators [30]-[34] and merchant operators [35]-[42].

For the former, from the viewpoint of the independent system operators, ES is integrated into the power system and acts as a reserve market participant to reduce power system costs. Many studies concentrate on how to establish the ES reserve model. Reference [30] presents an up-/down-reserve model that can be realized by increasing the discharging/charging level. In addition, the down/up discharging reserve models and down/up charging reserve models are considered in [31] to explicitly model the reserve contributions, as a supplement to the modes in [30]. Recognizing that ES can switch its operation statuses to provide up-/down-reserve, [32] and [33] propose a model to value the reserve provisioning ability of ES. Furthermore, when considering the actual SOC of ES, the multi-hour reserve deliverability constraint is considered. Reference [34] extends the formulations presented in [32] and [33] to compressed air ES and takes demand response into account. However, the feasibility of reserve capacity during each time period cannot be guaranteed in the above-mentioned studies because the reserve constraints do not consider SOC limits and do not guarantee the reserve deliverability constraints during all time periods. In addition, the function of ES as a reserve participant in [30]-[34] is similar to that of thermal units, compensating for generation deviations pertaining to the base scenario and all other unclear scenarios.

From the viewpoint of merchant operators [35]-[42], independent ES [35], [36] or joint systems involved with ES and RES [37] participates in the reserve auxiliary market from the viewpoint of merchant operators, and the goal is to maximize the profits of merchant operators. Reference [35] establishes an up-reserve provider model of independent ES, which is associated with ES discharging operation. In [36], an optimal scheduling model is proposed for a standalone ES to participate in multiple markets such as the reserve market. In [37], a coordinated strategy is proposed for a joint ES and wind power system in which ES can be used for the wind power accommodation, and the idle capacity and power of ES can be used to participate in the reserve ancillary market. It should be noted that in [35]-[37], a portion of the capacity is withheld as reserve capacity to prepare for future reserve demands. However, even without considering the feasibility of the methods themselves, the day-ahead reserve capacity provided by [35]-[37] is insufficient to guarantee dispatchability and will be infeasible in real-world applications. The reason is that reserve demand in real-time operation is not considered in [35], [37]. Consequently, there is a capacity deviation between the theoretical reserve capacity and the real reserve capacity due to the different real-time reserve deployments. The deviation will be accumulated and may violate the SOC boundaries. Though uncertain deployment of the reserve is considered in [36], the conservative strategy may greatly limit the opportunities of ES in reserve capacity.

The integration of ES into MG for participating in the day-ahead reserve market can be categorized into two groups. In the first group, MG with ES participates in the reserve market without considering the real-time scheduling constraints [38]-[40]. In [38], a deterministic energy and reserve scheduling method is established, which determines the total reserve demand of the grid before energy scheduling. Reference [39] establishes an innovative stochastic energy and reserve scheduling method for an MG. In [40], the scheduling problem of MGs is studied to participate in both energy and reserve markets with uncertainty injections, and a hybrid stochastic-information gap decision method is established. However, due to [38]-[40], without considering the real-time operation power balance, the discrepancy between the day-ahead market and real-time operation will be generated and exacerbated due to the uncertainties. In the second group, MG with ES participates in the reserve market considering the requirement of maintaining power balance in real-time operation [41], [42]. In [41], a two-stage SO method is provided for MGs taking part in joint day-ahead (energy and reserve) and real-time markets. The method in [41] has the capability of energy compensation in the real-time market. In [42], a multi-stage stochastic programming model is proposed to find the optimal offering strategy in energy and reserve markets. However, MG does not directly participate in the real-time energy scheduling in [41], [42]. Instead, its objective is to manage the power imbalance.

Accordingly, we intend to fill the gap that MG with ES is modeled as a reserve provider with consideration of the real-time scheduling process. However, there exists two problems. ① Can MG with ES realize optimal self-scheduling and reserve provision to other systems simultaneously without reserve service support from the main grid (the main grid just provides a determinized day-ahead energy curve)? ② If possible, how much day-ahead energy should the main grid provide and how much up-/down-reserve capacity can the MG system provide during each time period while guaranteeing the feasibility?

Thus, the significant contribution of this paper is to establish a novel day-ahead multi-stage RO reserve provision method for MG with ES to realize optimal self-scheduling and reserve provision to other external systems simultaneously. The original characteristics of this paper are summarized as follows.

1) From the viewpoint of the reserve provider, a day-ahead multi-stage RO reserve provision model is proposed with consideration of the actual scheduling process and the actual availability of provided reserves. In particular, real-time reserve demand is considered as uncertainty and is formulated as an adjustable uncertainty set. The upper bound of the uncertainty set (reserve capacity) is constructed as a decision variable and determined in day ahead. This type of uncertainty is known as decision-dependent uncertainty (or endogenous uncertainty). The multi-stage RO problem under decision-dependent uncertainty has not been studied [43].

2) The contract about the power injection curve from/to the main grid is signed in the day-ahead process. Thus, the main grid just provides constant/fixed energy to MG during each time period in the scheduling process, rather than a region, e.g., [13]-[22]. The main grid does not need to provide extra reserve service for the MG system to confront uncertainty.

3) The day-ahead up-/down-reserve capacity is determined such that there is always a feasible solution in the real-time scheduling for any realizations of uncertain up-/down-reserve demand (within the up-/down-reserve capacity).

Numerical tests conducted on a real MG with ES system verify the efficacy of the proposed model.

The remainder of this paper is organized as follows. In Section II, the framework and feasibility of MG with ES as a reserve provider are analyzed. Then a day-ahead multi-stage RO reserve provision model is established in Section III. Section IV provides an effective method to realize reserve provision. Section V implements numerical results, and Section VI provides the conclusion.

II. Framework and Feasibility of MG with ES as a Reserve Provider

A. Framework of MG with ES as a Reserve Provider

We aim to establish a day-ahead multi-stage RO reserve provision model for MG with ES under uncertainty, comprehensively considering the actual scheduling constraints and actual availability of provided reserves. Considering the low capacity of MG with ES in comparison with power systems or other market players, MG with ES participates in the market acting as a price-taker. The framework is shown in Fig. 1, which involves the day-ahead stage (in solid lines) and real-time stage (in dotted lines).

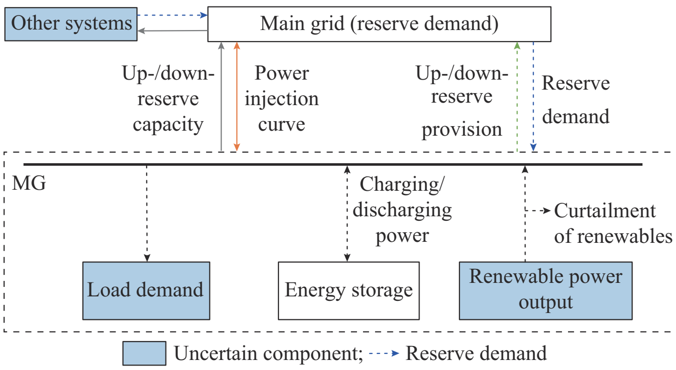

Fig. 1. Framework of MG with ES as a reserve provider.

The uncertainties include load demand, renewable power output as well as reserve demand. The decision variables can be divided into two categories based on different stages, namely day-ahead decision variables and real-time decision variables. The day-ahead decision variables include up-/down-reserve capacity to the main grid (in gray) and the power injection curve from/to the main grid (in orange). In addition, real-time decision variables include the up-/down-reserve provision to the main grid (in green) as well as the scheduling decisions of MG (in black) such as charging/discharging power of ES and curtailment of renewables. The scheduling process is described as follows.

In the day-ahead stage, MG with ES, as an independent reserve provider, will trade with the main grid in two aspects.

1) The first is the up-/down-reserve capacity provided to the main grid. Compared with other reserve provider methods in [35]-[42], the proposed method can give the maximum actual available up-/down-reserve capacity by considering the real-time scheduling requirements.

2) The second is the total power injection curve of MG with ES from/to the main grid, which is an important resource to satisfy the feasibility. Compared with the reserve-consumer model [13]-[22], the power injection curve in this paper is a deterministic curve determined in the day ahead rather than a specific region. It means that the exchange power between the MG and the main grid remains constant in the scheduling process and the main grid does not need to provide extra reserve service. Consequently, the scheduling difficulty and the burden of the main grid will be reduced.

With the fixed day-ahead decisions, real-time scheduling of MG with ES can realize optimal self-scheduling against any realization of uncertainties and can simultaneously provide reserve service for the main grid to meet the reserve demand within the determined reserve capacity.

B. Feasibility of MG with ES as a Reserve Provider: an Example

1) Feasibility of MG with ES as a Reserve Provider

In this part, we explore the potential of MG with ES, which has been operated as a reserve consumer in [13]-[22], to function as a reserve provider. To validate the hypothesis, a comparison example related to two cases is given. The parameters of MG with ES are shown in Table I.

TABLE I
PARAMETERS OF MG WITH ES

T (hour)	τ (hour)	$\bar{E}$ (MWh)	$\underline{E}$ (MWh)	E_0 (MWh)	$\bar{p}^{dis}$ (MW)	$\bar{p}^{ch}$ (MW)
3	1	11.4	3	7.2	3	3
η_d (%)	η_c (%)	$\bar{d}$ (MW)	$\underline{d}$ (MW)	$\bar{w}$ (MW)	$\underline{w}$ (MW)	
90	90	[5, 3, 7]	[3, 2, 6]	[5, 8, 4]	[4, 6, 3]	

Under the parameters in Table I, if the main grid can provide reserve capacity in the range of [−1, 1]MW during each time period, there will be feasible solutions to the economic scheduling problem, as supported by [44].

In the first case, MG with ES is regarded as a reserve consumer, and the main grid is required to provide reserve service to confront uncertainty. The method in [20] is selected as a representative method for MG with ES as a reserve consumer. According to [20], the safe range of ES level without considering reserve provision is shown in the orange area of Fig. 2, which is a necessary and sufficient condition to guarantee that the system has a feasible scheduling solution.

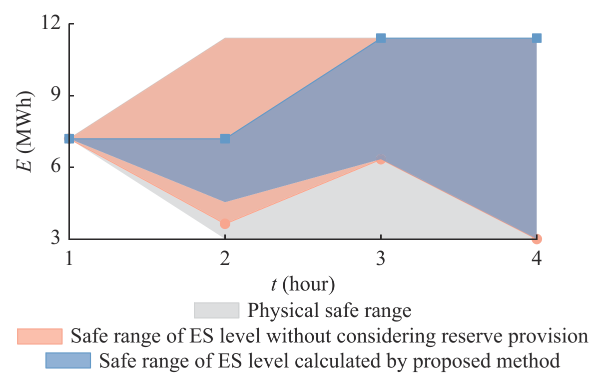

Fig. 2. Safe range under different conditions.

In the second case, our objective is to utilize the MG with ES to serve as a reserve provider. For the MG shown in Table I, if MG obtains −1 MW, 1 MW, and 1 MW energy from the main grid, MG can provide [2, 0, 0]MW up-reserve capacity and [0, 2, 0]MW down-reserve capacity to the main grid (or other external systems) while realizing self-scheduling. In other words, if the uncertain up-/down-reserve demands are within the up-/down-reserve capacities, MG with ES can also realize self-optimizing, which can be verified by [20]. Similarly, the safe range of ES level E calculated by the proposed method is shown in the blue area of Fig. 2.

From Fig. 2, it is noted that the safe ranges of ES level in both the first case and the second case are non-empty and smaller than the physical safe range. In other words, there will be feasible solutions for the given MG with ES both in the first case and the second case. Consequently, we can conclude that MG with ES has the potential to serve as a reserve provider under the suitable reserve capacity and power injection from the main grid.

2) Difference Analysis Between MG with ES as a Reserve-Provider and as a Reserve Consumer Through Example

Firstly, as shown in Fig. 2, the safe range of ES level in the second case is narrower compared with that in the first case. It is concluded that MG with ES as a reserve provider may reduce the feasible regions. It is reasonable because MG with ES as a reserve provider needs to address greater uncertainty, namely, uncertain up-/down-reserve demand. MG with ES needs to make a trade-off between economic feasibility and operational viability, which is also a key focus of our research.

Secondly, MG with ES in the first case needs [−1, 1]MW reserve capacity from the main grid and the corresponding reserve service. Instead, in the second case, MG with ES does not need reserve from the main grid (only [−1, 1, 1]MW determined power injection). Consequently, MG with ES as a reserve provider can reduce the burden of the main grid.

Thirdly, in the second case, extra [2, 0, 0]MW up-reserve capacity and [0, 2, 0]MW down-reserve capacity can be provided to the main grid.

Therefore, we can conclude that the given MG with ES as a reserve provider is feasible and meaningful.

III. Day-ahead Multi-stage RO Reserve Provision Model

The scheduling problem of MG as a reserve provider is also a multi-stage problem (the details refer to Section III-A). As discussed in Section I, the multi-stage RO method can be regarded as the most successful method for dealing with the multi-stage scheduling problem. Consequently, in this paper, a novel day-ahead multi-stage RO reserve provision model of MG with ES under uncertainty is established, which is different from the model in [19]-[22]. The solutions obtained by the model can satisfy device or contractual constraints under uncertainties without the reserve provided by the main grid.

A. Problem Description

According to the framework in Fig. 1, we know that the $R_t^+\left(R_t^-\right)$ is determined in the day-ahead process. Then, in the real-time process, $r^+\left(r^-\right)$ (within $\left[0, R_t^+\left(R_t^+\right)\right]$) can be dealt with by reasonably scheduling the equipment in the given MG system.

In other words, there is a coupling relationship between $r^+\left(r^-\right)$ and $R_t^+\left(R_t^-\right)$. Thus, $R_t^+\left(R_t^-\right)$ should be carefully decided to meet any realization of $r^+\left(r^-\right)$ while guaranteeing the feasibility of the real-time scheduling process. To this end, day-ahead scheduling should comprehensively consider the real-time scheduling process and requirements.

With the analysis of the framework and the operation requirements of MG with ES as a reserve provider in Fig. 1, it is known that the problem in this paper is a multi-stage scheduling problem. The sequential decision-making process is given in Fig. 3.

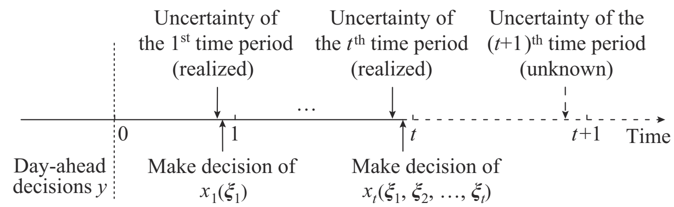

Fig. 3. Sequential decision-making process.

For a multi-stage scheduling problem, two important requirements are nonanticipativity and multi-stage robustness. These requirements have been recognized in many studies [19] - [22], [25] - [28]. In particular, nonanticipativity means that the current decision can be only made based on the realization information up to the current time period. Multi-stage robustness necessitates that the solutions will be viable for any possible realization of uncertainty within the given uncertainty set [45].

To be specific, the uncertainty realization information of each period is unknown in the day-ahead stage. R_t^+ and R_t^- should be made only based on the information of uncertainty sets for $t = 1, 2, \ldots, T$, referring to the nonanticipativity requirement. But at the same time, R_t^+ and R_t^- should be feasible for any realization of r_t^+ and r_t^- in real-time operation, which is multi-stage robustness.

In the real-time stage, day-ahead solutions $R_t^+\left(R_t^-\right)$ are fixed. And real-time decisions x_t during time period t should be made only relying on x_v $\left(v = 1, 2, \ldots, t-1\right)$, the observed uncertainty parameters such as load demand d_s, wind power outputs w_s, photovoltaic power outputs p_s^{PV} $\left(s = 1, 2, \ldots, t\right)$, and the reserve demand $r_u^+\left(r_u^-\right)$ $\left(u = 1, 2, \ldots, t\right)$ within $R_t^+\left(R_t^-\right)$. Consequently, decisions x_t can be denoted as $x_t\left(\boldsymbol{\xi}_{[t]}\right)$, where $\boldsymbol{\xi}_{[t]} = [\boldsymbol{d}_{[t]}; \boldsymbol{w}_{[t]}; \boldsymbol{p}_{[t]}^{\mathrm{PV}}; \boldsymbol{r}_{[t]}^+; \boldsymbol{r}_{[t]}^-]$, $\boldsymbol{d}_{[t]} = (d_1, d_2, \ldots, d_t)$, $\boldsymbol{w}_{[t]} = \left(w_1, w_2, \ldots, w_t\right)$, $\boldsymbol{p}_{[t]}^{\mathrm{PV}} = \left(p_1^{\mathrm{PV}}, p_2^{\mathrm{PV}}, \ldots, p_t^{\mathrm{PV}}\right)$, $\boldsymbol{r}_{[t]}^+ = \left(r_1^+, r_2^+, \ldots, r_t^+\right)$, and $\boldsymbol{r}_{[t]}^- = \left(r_1^-, r_2^-, \ldots, r_t^-\right)$ are the vectors of uncertainty up to time t. In addition, $x_t\left(\boldsymbol{\xi}_{[t]}\right)$ should satisfy the real-time scheduling constraints to guarantee that the solution is feasible.

Based on the above analysis, the day-ahead reserve provision model should be established as a multi-stage RO model. And the detailed description is shown below.

B. Uncertainty Description

In RO method, uncertainties are often modeled by the uncertainty sets. The detailed description of uncertainties is given below.

Specifically, uncertainties in the problem involve w_t, p_t^{PV}, d_t, r_t^+, and r_t^-. According to the characteristics, the uncertainties can be divided into two categories.

The first category includes w_t, p_t^{PV}, and d_t, which are simulated via uncertainty sets in (1)-(3), respectively. The bounds of w_t, p_t^{PV}, and d_t are usually predicted parameters and can be obtained by the data-driven method [46] based on historical data.

$$w=\left\{w_t \middle| \underline{w}_t \leq w_t \leq \bar{w}_t\right\} \quad \forall t \tag{1}$$

$$p^{\mathrm{PV}}=\left\{p_t^{\mathrm{PV}} \middle| \underline{p}_t^{\mathrm{PV}} \leq p_t^{\mathrm{PV}} \leq \bar{p}_t^{\mathrm{PV}}\right\} \quad \forall t \tag{2}$$

$$d=\left\{d_t \middle| \underline{d}_t \leq d_t \leq \bar{d}_t\right\} \quad \forall t \tag{3}$$

The second category includes r_t^+ and r_t^-. Different from uncertainty sets in the first category whose bounds are certain predicted constant parameters based on the real data, the bounds (capacities) of $R_t^+\left(R_t^-\right)$ in the second category uncertainty set is in fact artificially given parameters in the day-ahead. Thus, $R_t^+\left(R_t^-\right)$ should be carefully determined to satisfy real-time scheduling requirements.

To this end, in this paper, R_t^+ and R_t^- have been defined as decision variables, and thus, the uncertainty sets of r_t^+ and r_t^- are described in (4) and (5), respectively.

$$r^+=\left\{r_t^+ \middle| 0 \leq r_t^+ \leq R_t^+\right\} \quad \forall t \tag{4}$$

$$r^-=\left\{r_t^- \middle| 0 \leq r_t^- \leq R_t^-\right\} \quad \forall t \tag{5}$$

Equations (4) and (5) should be added to the day-ahead multi-stage RO reserve provision model in (8)-(18) as significant constraints. Once day-ahead R_t^+ and R_t^- are decided, all the r_t^+ and r_t^- should be confronted when r_t^+ and r_t^- vary within R_t^+ and R_t^-.

For brevity, the uncertainty set in this paper can be unified as Ω:

$$\Omega=\left\{\boldsymbol{\xi} \in R^T \middle| (1)\text{-}(5)\right\} \tag{6}$$

where $\boldsymbol{\xi}=\left(\boldsymbol{\xi}_1, \boldsymbol{\xi}_2, \ldots, \boldsymbol{\xi}_T\right)$.

Besides, during time period t, $\boldsymbol{\xi}_1, \boldsymbol{\xi}_2, \ldots, \boldsymbol{\xi}_t$ are known, therefore, the uncertainty set can be updated. Consequently, conditional uncertainty set $\Omega_t\left(\boldsymbol{\xi}_{[t]}\right)$ is introduced to provide a more accurate depiction of the temporal evolution of the uncertainty set. $\Omega_t\left(\boldsymbol{\xi}_{[t]}\right)$ is abbreviated as Ω_t in the latter part for convenience.

$$\Omega_t\left(\boldsymbol{\xi}_{[t]}\right)=\left\{\boldsymbol{\xi}_{t+1}, \boldsymbol{\xi}_{t+2}, \ldots, \boldsymbol{\xi}_T \middle| \boldsymbol{\xi} \in \Omega\right\} \tag{7}$$

C. Mathematical Formulation

We aim to realize that MG with ES can schedule its internal resources to provide reserve service to other systems and maintain the security and reliability of self-scheduling under uncertainties. In the scheduling problem, the day-ahead decision variables include power injection from/to the main grid $\tilde{d}$, and up-/down-reserve capacity $R^+(R^-)$. Besides, the real-time decision variables include charging/discharging power of ES p^{sto}, curtailment of wind power outputs w^{cur}, and curtailment of photovoltaic power outputs p^{PVcur}. Based on the analysis in Section III-A, decisions should be denoted as the functions of uncertainty up to time t (or the functions of $\boldsymbol{\xi}_{[t]}$) due to the nonanticipativity requirement. Moreover, according to the multi-stage robustness requirement, decisions should satisfy the scheduling constraints to guarantee the solutions viable for any possible realization of uncertainty within the given uncertainty set.

To this end, conceptually, a new single-level day-ahead multi-stage RO reserve provision model is developed in (8)-(18). The objective function (8) is to minimize the weighted sum of operation costs. The first and second terms in (8) correspond to the cost related to the power injection from the main grid and the profit related to the reserve provision to the main grid, respectively.

$$\begin{aligned}\min_{\substack{\tilde{d}_t, R_t^+, R_t^-, p_t^{\mathrm{sto}}, \\ w_t^{\mathrm{cur}}, p_t^{\mathrm{PVcur}}}} & \sum_{t=1}^{T} \tau\left(\lambda_t^+ \max\left(\tilde{d}_t, 0\right)+\lambda_t^- \min\left(\tilde{d}_t, 0\right)\right)- \\ & \sum_{t=1}^{T}\left(\mu_t^+ R_t^+ + \mu_t^- R_t^-\right)\end{aligned} \tag{8}$$

In addition, the constraints are cast as in (9)-(18).

$$\begin{aligned}p_t^{\mathrm{sto}}\left(\boldsymbol{\xi}_{[t]}\right)+w_t-w_t^{\mathrm{cur}}\left(\boldsymbol{\xi}_{[t]}\right)+p_t^{\mathrm{PV}}-p_t^{\mathrm{PVcur}}\left(\boldsymbol{\xi}_{[t]}\right)+ \\ \tilde{d}_t=d_t-r_t^+ + r_t^- \quad \forall t, \boldsymbol{\xi} \in \Omega_t\end{aligned} \tag{9}$$

$$-\bar{p}_t^{\mathrm{ch}} \leq p_t^{\mathrm{sto}}\left(\boldsymbol{\xi}_{[t]}\right) \leq \bar{p}_t^{\mathrm{dis}} \quad \forall t, \boldsymbol{\xi} \in \Omega_t \tag{10}$$

$$\underline{E}_t \leq E_t\left(\boldsymbol{\xi}_{[t]}\right) \leq \bar{E}_t \quad \forall t, \boldsymbol{\xi} \in \Omega_t \tag{11}$$

$$E_t\left(\boldsymbol{\xi}_{[t]}\right)-E_{t-1}\left(\boldsymbol{\xi}_{[t-1]}\right)=h\left(p_t^{\mathrm{sto}}\left(\boldsymbol{\xi}_{[t]}\right)\right) \quad \forall t, \boldsymbol{\xi} \in \Omega_t \tag{12}$$

$$\begin{cases} h(x)=-\left(\tau/\eta_d\right)\max\{x, 0\}-\tau\eta_c \min\{x, 0\} \\ h^{-1}(x)=-\left(\eta_d/\tau\right)\min\{x, 0\}-\left(1/\left(\eta_c\tau\right)\right)\max\{x, 0\} \end{cases} \tag{13}$$

$$0 \leq w_t^{\mathrm{cur}}\left(\boldsymbol{\xi}_{[t]}\right) \leq w_t \quad \forall t, \boldsymbol{\xi} \in \Omega_t \tag{14}$$

$$0 \leq p_t^{\mathrm{PVcur}}\left(\boldsymbol{\xi}_{[t]}\right) \leq p_t^{\mathrm{PV}} \quad \forall t, \boldsymbol{\xi} \in \Omega_t \tag{15}$$

$$0 \leq R_t^+ \tag{16}$$

$$0 \leq R_t^- \tag{17}$$

$$\underline{g}_t \leq \tilde{d}_t + r_t^+ - r_t^- \leq \bar{g}_t \tag{18}$$

Equation (9) describes the power balance constraints. Constraints (10)-(13) are related to ES, where (10) is the bounds on charging/discharging power, and (11) is the bound limit of ES level. Equation (12) is the evolution equation of ES level, where $h(\cdot)$ and its inverse $h^{-1}(\cdot)$ are auxiliary functions [20], denoted in (13). In addition, the characteristics of $h(\cdot)$ and its inverse $h^{-1}(\cdot)$ such as monotonicity and piecewise linear, can provide convenience for the following research. Constraints (14) and (15) describe the curtailment limit of wind power outputs and photovoltaic power outputs, respectively. Constraints (16) and (17) restrict that up- and down-reserve capacities should be positive.

Constraint (18) corresponds to the power exchange limits between the MG and the main grid. If MG with ES purchases energy from the main grid, the power transfer value $\tilde{d}_t$ will be positive. Conversely, if MG with ES provides power to the main grid, $\tilde{d}_t$ will be negative.

Except constraints (16) and (17), it is noted that (18) is one of the main differences between the proposed model and the reserve consumer model [13]-[22]. In this paper, $\tilde{d}_t$ is determined in the day-ahead stage and remains constant during time period t in the real-time stage ($t=1,2,\ldots,T$) such that $\tilde{d}_t$ is within a curve rather than a region. In other words, the exchange power between the MG and the main grid keeps in a determinized curve, which can reduce the scheduling difficulty of the main grid.

Differently, MG with ES is regarded as a reserve consumer in [13]-[22] because power injection from/to the main grid in [13]-[22] is a real-time decision and is within the power exchange limits. Consequently, the main grid will provide extra reserve capacity to satisfy the real-time scheduling problem, which will increase the burden of the main grid.

IV. Multi-stage Robust Optimization Method

A. Difficulty Analysis

With the analysis in Section III-A, the day-ahead multi-stage scheduling process of MG with ES as a reserve provider is established, comprehensively considering the feasibility of the real-time scheduling requirements. Real-time decision variables $p_t^{\mathrm{sto}}\left(\boldsymbol{\xi}_{[t]}\right)$, $w_t^{\mathrm{cur}}\left(\boldsymbol{\xi}_{[t]}\right)$, and $p_t^{\mathrm{PVcur}}\left(\boldsymbol{\xi}_{[t]}\right)$ as well as real-time state variable $E_t\left(\boldsymbol{\xi}_{[t]}\right)$ during time period t in the proposed model only depend on $\boldsymbol{\xi}_{[t]}$ (realization information of uncertainties up to time period t) such that real-time decisions satisfy the nonanticipativity requirement. However, the model in (8)-(18) is just a descriptive model and is unsolvable. In fact, the model includes an infinite number of constraints. To ensure that the obtained solutions are feasible for all uncertainty realizations, all of the constraints should be satisfied.

In other words, the major challenge is how to obtain feasible reserve provision solutions during each time period that can satisfy the operation constraints under any realizations of uncertainties, which corresponds to the multi-stage robustness requirement.

B. Multi-stage Robust Feasible Regions

From the mathematical viewpoint, the concept of multi-stage robustness means: during the current time period t, state variable E_t and real-time decision variables x_t should be determined by the day-ahead decisions y, E_{t-1} at the end of time period $t-1$, and the observed uncertain vector $\boldsymbol{\xi}_t$ during time period t. The relationship can be described as $\left(E_t,x_t\right)\in\Psi\left(y,E_{t-1},\xi_t\right)$. Thus, multi-stage robustness implies that $\Psi\left(y,E_{t-1},\xi_t\right)$ is non-empty for any $\boldsymbol{\xi}_t$. The conclusion can be extended to the whole time. Then, based on the analysis above, we first define the multi-stage robust feasible region for model (8)-(18).

Definition 1: the multi-stage robust feasible region $\mathcal{F}_{t-1}$ for state variables is illustrated in (19).

$$\mathcal{F}_{t-1}=\left\{E_{t-1}\in\left[\underline{E}_{t-1},\bar{E}_{t-1}\right]\middle|\forall\xi_t\in\Omega_t,\Psi\left(y,E_{t-1},\xi_t\right)\neq\varnothing\right\} \tag{19}$$

$$\Psi\left(y,E_{t-1},\xi_t\right)=\left\{\left(y,E_t,x_t\right)\middle|\, y,\ E_t,\text{ and } x_t \text{ limited by (9)-(18)}, E_t\in\mathcal{F}_t\right\} \tag{20}$$

Then, the original problem is transformed into how to obtain the feasible solution region for each time period. Then, an important proposition is given to describe the regions of the feasible solutions that can satisfy nonanticipativity and multi-stage robustness simultaneously.

Proposition 1: if the precondition (21) is satisfied and $\mathcal{F}_{t-1}=\left[\underline{E}_{t-1}^{\mathrm{true}},\bar{E}_{t-1}^{\mathrm{true}}\right]$ in (22) is not empty, there is always a feasible solution to (8)-(18) if E_{t-1} is within the multi-stage robust feasible region $\mathcal{F}_{t-1}=\left[\underline{E}_{t-1}^{\mathrm{true}},\bar{E}_{t-1}^{\mathrm{true}}\right]$.

$$\begin{cases}-\tilde{d}_t+\underline{d}_t-R_t^+\geq-\bar{p}_t^{\mathrm{ch}}\\ \bar{p}_t^{\mathrm{dis}}\geq-\underline{w}_t-\underline{p}_t^{\mathrm{PV}}-\tilde{d}_t+\bar{d}_t+R_t^-\end{cases} \tag{21}$$

$$\begin{cases}\bar{E}_{t-1}^{\mathrm{true}}=\min\left\{\bar{E}_t^{\mathrm{true}}-h\left(-\tilde{d}_t+\underline{d}_t-R_t^+\right),\bar{E}_t^{\mathrm{true}}-h\left(\bar{p}_t^{\mathrm{dis}}\right),\bar{E}_{t-1}\right\}\\ \underline{E}_{t-1}^{\mathrm{true}}=\max\left\{\underline{E}_t^{\mathrm{true}}-h\left(-\underline{w}_t-\underline{p}_t^{\mathrm{PV}}-\tilde{d}_t+\bar{d}_t+R_t^-\right),\right.\\ \qquad\left.\underline{E}_t^{\mathrm{true}}-h\left(-\bar{p}_t^{\mathrm{ch}}\right),\underline{E}_{t-1}\right\}\end{cases} \tag{22}$$

The details of proof of Proposition 1 can be located in the Appendix A.

Based on Proposition 1, it is known that:

1) There is a nonanticipative and multi-stage robust solution if $\mathcal{F}_{t-1}=\left[\underline{E}_{t-1}^{\mathrm{true}},\bar{E}_{t-1}^{\mathrm{true}}\right]$ is non-empty during all time periods. Consequently, (23) should be satisfied to ensure the nonanticipativity and multi-stage robustness of the solution.

$$\underline{E}_t^{\mathrm{true}}\leq\bar{E}_t^{\mathrm{true}}\quad\forall t\in T \tag{23}$$

2) Constraint (22) reveals the coupling relationship of the feasible region between two adjacent periods. To ensure all-time-period feasibility, the energy level of ES at each end of the time period t ($t=1,2,\ldots,T$) should be within the feasible region. Consequently, the formulation (22) is a set of constructive constraints that would be introduced into the day-ahead multi-stage RO reserve provision model (24)-(33).

3) Auxiliary functions $h(\cdot)$ and its inverse $h^{-1}(\cdot)$ (13) as well as nonlinear constraint (22) can be transformed into linear formulations by using linear techniques such as the big-M method, and (13) and (22) will be solved by commercial solvers.

C. Day-ahead Optimal Scheduling Model

Proposition 1 gives the condition to obtain the feasible regions, which can make the proposed problem tractable under uncertainties. Based on Proposition 1, the day-ahead decisions for guaranteeing the feasibility scheduling of MG with ES under uncertainties can be obtained by solving the following problem.

$$\min_{\substack{\tilde{d}_t,R_t^+,R_t^-\\ \bar{E}_t^{\mathrm{true}},\underline{E}_t^{\mathrm{true}}}}\sum_{t=1}^{T}\tau\left(\lambda_t^+\max\left(\tilde{d}_t,0\right)+\lambda_t^-\min\left(\tilde{d}_t,0\right)\right)-\sum_{t=1}^{T}\left(\mu_t^+R_t^++\mu_t^-R_t^-\right) \tag{24}$$

$$\underline{g}_t\leq\tilde{d}_t+R_t^+\leq\bar{g}_t\quad\forall t\in T \tag{25}$$

$$\underline{g}_t\leq\tilde{d}_t-R_t^-\leq\bar{g}_t\quad\forall t\in T \tag{26}$$

$$0\leq R_t^+\quad\forall t\in T \tag{27}$$

$$0\leq R_t^-\quad\forall t\in T \tag{28}$$

$$-\tilde{d}_t + \underline{d}_t - R_t^+ \ge -\bar{p}_t^{\text{ch}} \quad \forall t \in T \tag{29}$$

$$\bar{p}_t^{\text{dis}} \ge -\underline{w}_t - \underline{p}_t^{\text{PV}} - \tilde{d}_t + \bar{d}_t + R_t^- \quad \forall t \in T \tag{30}$$

$$\underline{E}_t^{\text{true}} \le \bar{E}_t^{\text{true}} \quad \forall t \in T \tag{31}$$

$$\bar{E}_{t-1}^{\text{true}} = \min\left\{\bar{E}_{t-1}, \bar{E}_t^{\text{true}} - h\left(\bar{p}_t^{\text{dis}}\right), \bar{E}_t^{\text{true}} - h\left(-\tilde{d}_t + \underline{d}_t - R_t^+\right)\right\} \quad \forall t \in T \tag{32}$$

$$\underline{E}_{t-1}^{\text{true}} = \max\left\{\underline{E}_{t-1}, \underline{E}_t^{\text{true}} - h\left(-\bar{p}_t^{\text{ch}}\right), \underline{E}_t^{\text{true}} - h\left(-\underline{w}_t - \underline{p}_t^{\text{PV}} - \tilde{d}_t + \bar{d}_t + R_t^-\right)\right\} \quad \forall t \in T \tag{33}$$

The purpose of the day-ahead multi-stage RO reserve provision model (24) - (33) is to obtain the power injection curve, the up-/down-reserve capacity, and feasible/safe regions of the energy level of ES. The objective function (24) aims to minimize the total operation cost. Constraints (25) and (26) restrict that the power injection is within the limitations. Constraints (27) and (28) require that the up-capacity and down-capacity are positive. Constraints (29) and (30) are preconditions and the system has no feasible solution if the precondition is not satisfied. Constraints (31) - (33) describe the feasible regions of ES for satisfying nonanticipativity as well as multi-stage robustness.

Compared with the original stochastic programming problem (8)-(18), formulations (24)-(33) can be converted into a mixed-integer linear programming (MILP) problem and thus will be solved directly by commercial solvers such as Gurobi.

D. Overall Schematic Diagram

With the above-mentioned analysis, the schematic diagram of the day-ahead multi-stage RO reserve provision method can be summarized in Fig. 4, and two parts are included. The first process is the precondition, which aims to construct the feasible region-related constraints that can satisfy nonanticipativity and multi-stage robustness based on Proposition 1. The input data are the upper and lower bounds of uncertainty sets and the output is the constraint function (21) and (22).

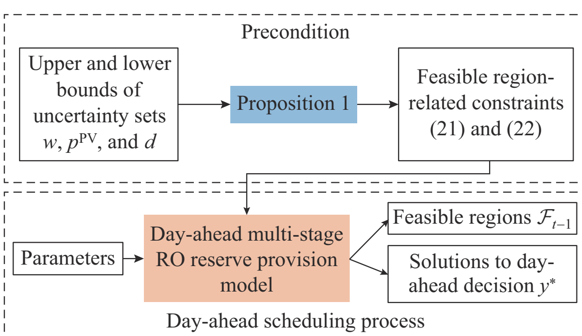

Fig. 4. Schematic diagram of day-ahead multi-stage RO reserve provision method.

Then, based on these constraints, the day-ahead multi-stage RO reserve provision model (24)-(33) is applied under the given parameters such that optimal day-ahead solutions can be obtained (including the exact day-ahead feasible regions for ES energy level, $R_t^+(R_t^-)$, and power injection curve during each time period). In this way, there is always a feasible economic scheduling solution to any realizations of real-time up-/down-reserve demand within the reserve capacity $\left[0, R_t^+(R_t^-)\right]$ and any realization of the first-category uncertainties.

V. Numerical Tests

Numerical tests are implemented on an MG with ES to confirm the effectiveness of the proposed method. The simulations are conducted using MATLAB R2020b and Gurobi 9.1.2 on a desktop computer.

A. Basic Information

To show the effectiveness of the proposed model, MG with a 2 MW wind farm, a 2.5 MW photovoltaic unit, and an ES is given. The load demand data (as shown in Fig. 5), the wind power output (as shown in Fig. 6), and the photovoltaic power output (as shown in Fig. 7) of the system come from a real area. The parameters of ES are detailed in Table II.

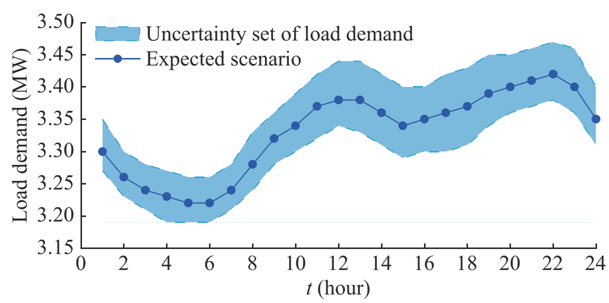

Fig. 5. Bounds of load demand and its corresponding expected scenario.

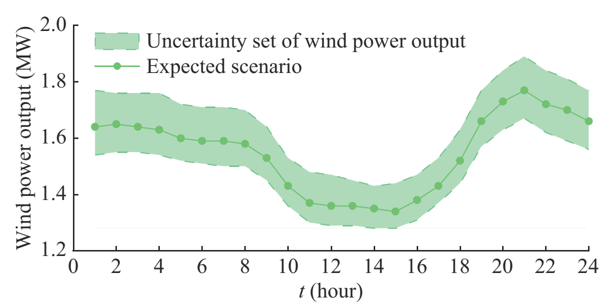

Fig. 6. Bounds of wind power output and its corresponding expected scenario.

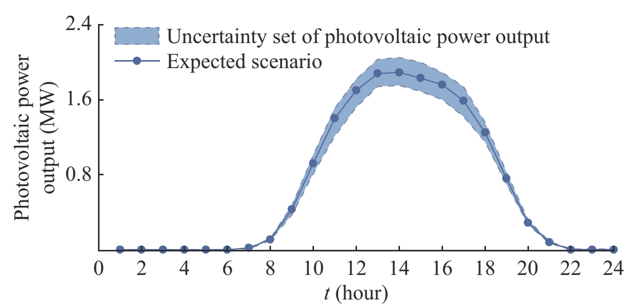

Fig. 7. Bounds of photovoltaic power output and its corresponding expected scenario.

TABLE II
PARAMETERS OF ES

$\bar{E}$ (MWh)	$\underline{E}$ (MWh)	E_0 (MWh)	$\bar{p}^{\mathrm{dis}}$ (MW)	$\bar{p}^{\mathrm{ch}}$ (MW)	η_c (%)	η_d (%)
7.6	2	4.8	2	2	90	90

B. Performance of Proposed Method

Then, the performance of the proposed method is examined and the testing results are shown in Fig. 8. From Fig. 8, the power injection is determined in the day-ahead stage and is applied in the real-time process. In this case, it is calculated that there is no feasible solution if the power injection is zero. This means that the power injection is necessary for the stability of the system under uncertainties. This is because ES can only transfer the energy and cannot generate sufficient energy to fill the difference between the wind power output and the load demand during the whole time period. In addition, from the trend of the power injection curve, we can notice that MG tends to purchase electricity from the main grid (positive power injection) when the PJM market electricity price is low and vice versa. It proves that the proposed method is effective.

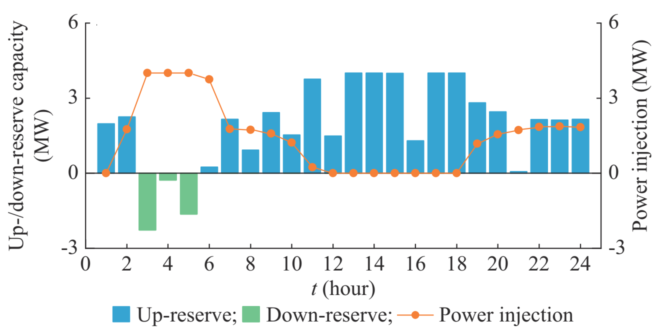

Fig. 8. Day-ahead reserve capacity and power injection results of proposed method.

Day-ahead up-reserve capacity and down-reserve capacity to the main grid are calculated and are also depicted in Fig. 8. From Fig. 8, the reserve capacity is substantially given by MG with ES, which means that MG with ES has great potential in providing reserve services. For any uncertain up-/down-reserve demand within the reserve capacity, the MG system can find a feasible solution to handle it through the proposed method.

Further, the feasible regions of ES are shown in Fig. 9, which is a sufficient condition to ensure the feasibility of the obtained solutions. The regions are included in the physical bounds of the ES level due to the operation constraints, especially the coupling constraints. We can know that the feasible regions are non-empty in this case such that there is always a feasible solution of the MG with ES satisfying all the constraints and confronting any realization of uncertainties. It is convenient and safe for the operators because they just need to choose suitable decisions within the regions for each time period to cope with the complex constraints and uncertainties of the system.

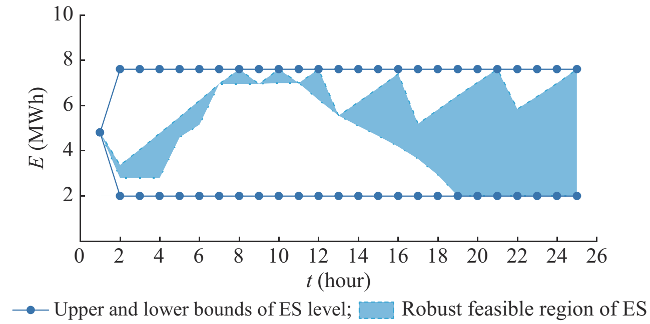

Fig. 9. Feasible regions for ES.

In addition, the performance of the proposed method is examined in real-time scheduling in various representative scenarios. Additionally, an ex-post analysis is conducted to demonstrate the practicability of the proposed method. Six representative and complex combination scenarios are selected, including the selected vertex scenarios (scenario 1 and scenario 2), the base scenario (scenario 3), two kinds of extreme ramping scenarios (scenario 4 and scenario 5), as well as one scenario generated by the Monte Carlo method (scenario 6). The real-time scheduling model is to minimize the total curtailment of wind power output and photovoltaic power output while subject to constraints (9)-(10), (12)-(15) and $\underline{E}_t^{\mathrm{true}} \leq E_t \leq \bar{E}_t^{\mathrm{true}}$. The real-time scheduling process is a typical structure of multi-stage decision process. Thus, the real-time scheduling model is applied via a rolling horizon framework with the objective of minimizing the total curtailment of wind power output and photovoltaic power output.

The performance in these scenarios is analyzed and the results are shown in Fig. 10, which shows that ES levels in different scenarios are all within the robust feasible region and the physical upper and lower bounds. Consequently, the boundaries are always met such that feasibility is always achieved.

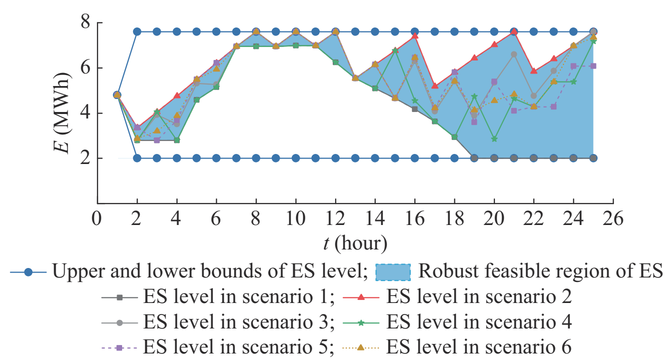

Fig. 10. ES levels in different scenarios.

C. Profits of ES when Participating in Reserve Provision

Then, we analyze the impact on the economy of the system when MG with ES participates in the reserve auxiliary market. The parameters are referred to Section V-A. The settings for the case studies and the comparison results are shown in Table III. To be specific, in case 1, there is no ES equipped in the MG system, which means the ES will not participate in either the energy market (self-scheduling) or the reserve auxiliary market (reserve provision). In case 2, ES is added to the MG system to gain profits from the energy market. In case 3, ES in MG is applied in both the self-scheduling and reserve provision to the main grid based on the proposed method.

TABLE III
SETTINGS FOR CASE STUDIES AND COMPARISON RESULTS

Case	Energy market	Reserve auxiliary market	Cost ($)	Cost saving rate (%)
1	No	No	836.99	
2	Yes	No	668.98	20.07
3	Yes	Yes	24.53	97.07

With the analysis of the costs under these three different cases, it is noted that the cost in case 1 is higher than that in other cases. In case 2, the cost of MG with ES will decrease by 20.07% than that in case 1 and will reach $668.98. The reason is that ES in MG can discharge and charge according to the electricity price to provide flexibility and improve the economy of the system. As for case 3, ES in MG is applied in both the self-scheduling and reserve provision to the main grid under the proposed method. The total cost is significantly reduced by 97.07% than that of case 1 and reaches $24.53.

The results mean that ES in MG can decrease the operation cost by joint self-scheduling and reserve provision, especially by reserve provision. Consequently, it is economical to use MG with ES as a reserve provider.

D. Comparison and Analysis

This model is compared with the reserve provision model in [33] from three aspects, including feasibility, optimality, and efficiency. To ensure comparability, the system in [33] is also equipped with a 2 MW wind farm, a 2.5 MW photovoltaic unit, and an ES, and the power injection varies within [1.2, 4]MW. Other parameters are also consistent with Section V-A. Then, the comparison results are shown in Table IV.

TABLE IV
COMPARISON RESULTS

Method	Total cost ($)	Calculation time (s)
Proposed method	–153.94	0.33
Reserve provider method in [33] (3 scenarios)	904.13	0.91
Reserve provider method in [33] (10 scenarios)	907.90	11.79
Reserve provider method in [33] (50 scenarios)	909.05	42.28

1) Feasibility analysis. The scheduling problem in this paper is solved by the day-ahead multi-stage RO reserve provision method. Consequently, the solutions obtained by the proposed method can always be feasible for any realization of uncertainties because nonanticipativity and multi-stage robustness requirements are satisfied. Differently, the problem in [33] is solved by the scenario-based method such that the feasibility of the finite selected scenarios can be guaranteed. In addition, the method in [33] can only satisfy the four-hour running requirement for ES while the proposed method in this paper can satisfy the running requirement for the entire periods.

2) Optimality analysis. From Table IV, the total cost obtained by the proposed method is $−153.94, which is lower than that in [33]. Consequently, it is concluded that the proposed method has better economic performance than that in [33]. The reason is that MG with ES can not only guarantee the feasibility under uncertainties based on the proposed method but also provide reserve auxiliary service to the main grid such that extra income can be obtained. In addition, the total cost of the scenario-based method is associated with the number of scenarios and it will increase with the number of scenarios. Consequently, more reserve capacities should be given to handle the more uncertain scenarios.

3) Efficiency analysis. Table IV shows that the calculation time of the proposed method is less than that in [33], which means that the proposed method has better efficiency than that in [33]. This is because the uncertainty can be solved in this paper by the maximum and minimum limits of the uncertainty set according to Proposition 1, rather than the specific scenarios like the scenario-based method.

VI. CONCLUSION

This paper investigates the feasibility and economy of MG with ES in reserve provision. A day-ahead multi-stage RO reserve provision model is established against the uncertainties comprehensively considering the real-time scheduling and reserve requirements. An effective method is given based on the structure of the constraint such that the original complex scheduling problem can be converted into an MILP problem and directly solved.

Numerical tests are implemented and the results show that: ① compared with the reserve consumer method, the proposed method can provide a reserve to other systems such that the total costs under the proposed method will be greatly reduced; ② compared with other provision methods, the proposed method has more advantages in terms of feasibility, optimality, and efficiency. Further work will analyze the potential of the proposed method in planning the location of ES from an economic viewpoint.

APPENDIX A

Proof of Proposition 1: for brevity, real-time decision variables are abbreviated as:

$$\begin{cases} P_t^{\text{sto}} = P_t^{\text{sto}}\left(\xi_{[t]}\right) \\ w_t^{\text{cur}} = w_t^{\text{cur}}\left(\xi_{[t]}\right) \\ p_t^{\text{PVcur}} = p_t^{\text{PVcur}}\left(\xi_{[t]}\right) \end{cases} \tag{A1}$$

To simplify the structure of the constraints and facilitate the analysis, E_t is selected as the main variable. Then, p_t^{sto},

w_t^{cur}, and p_t^{PVcur} can be substituted. The details are as follows.

First, p_t^{sto} can be equivalent to (A2) according to (12) and (13).

$$p_t^{\text{sto}} = h^{-1}\left(E_t - E_{t-1}\right) \tag{A2}$$

With (10), (A2), and $h^{-1}(\cdot)$ function with monotonically decreasing characteristics, we can obtain:

$$h\left(\bar{p}_t^{\text{dis}}\right) + E_{t-1} \le E_t \le h\left(-\bar{p}_t^{\text{ch}}\right) + E_{t-1} \tag{A3}$$

Similarly, w_t^{cur} can be represented as (A4) by (9) and (A2).

$$\begin{aligned} w_t^{\text{cur}} &= p_t^{\text{sto}} + w_t + p_t^{\text{PV}} - p_t^{\text{PVcur}} + \tilde{d}_t - d_t + r_t^+ - r_t^- = \\ &h^{-1}\left(E_t - E_{t-1}\right) + w_t + p_t^{\text{PV}} - p_t^{\text{PVcur}} + \tilde{d}_t - d_t + r_t^+ - r_t^- \end{aligned} \tag{A4}$$

Constraint (14) can be transferred as (A5) with (A4).

$$\begin{cases} 0 \le h^{-1}\left(E_t - E_{t-1}\right) + w_t + p_t^{\text{PV}} - p_t^{\text{PVcur}} + \tilde{d}_t - d_t + r_t^+ - r_t^- \\ h^{-1}\left(E_t - E_{t-1}\right) + p_t^{\text{PV}} - p_t^{\text{PVcur}} + \tilde{d}_t - d_t + r_t^+ - r_t^- \le 0 \end{cases} \tag{A5}$$

Reorganize (A5), and we can obtain:

$$\begin{cases} p_t^{\text{PVcur}} \le h^{-1}\left(E_t - E_{t-1}\right) + w_t + p_t^{\text{PV}} + \tilde{d}_t - d_t + r_t^+ - r_t^- \\ h^{-1}\left(E_t - E_{t-1}\right) + p_t^{\text{PV}} + \tilde{d}_t - d_t + r_t^+ - r_t^- \le p_t^{\text{PVcur}} \end{cases} \tag{A6}$$

With (15) and (A6), the constraints that guarantee the non-empty of p_t^{PVcur} are listed in (A7).

$$\begin{cases} 0 \le h^{-1}\left(E_t - E_{t-1}\right) + w_t + p_t^{\text{PV}} + \tilde{d}_t - d_t + r_t^+ - r_t^- \\ h^{-1}\left(E_t - E_{t-1}\right) + \tilde{d}_t - d_t + r_t^+ - r_t^- \le 0 \end{cases} \tag{A7}$$

Reorganize (A7) with $E_t - E_{t-1}$, and there will be:

$$\begin{cases} h\left(-\tilde{d}_t + d_t - r_t^+ + r_t^-\right) + E_{t-1} \le E_t \\ E_t \le h\left(-w_t - p_t^{\text{PV}} - \tilde{d}_t + d_t - r_t^+ + r_t^-\right) + E_{t-1} \end{cases} \tag{A8}$$

Consequently, constraints related to w_t^{cur}, p_t^{PVcur}, and p_t^{sto} can be converted into the constraints related to $E_t - E_{t-1}$ such that w_t^{cur}, p_t^{PVcur}, and p_t^{sto} can be omitted.

For brevity, (A9) is introduced.

$$\begin{cases} \bar{f}_t = \left\{\bar{E}_t, h\left(-\bar{p}_t^{\text{ch}}\right) + E_{t-1}, h\left(-w_t - p_t^{\text{PV}} - \tilde{d}_t + d_t - r_t^+ + r_t^-\right) + E_{t-1}\right\} \\ \underline{f}_t = \left\{\underline{E}_t, h\left(\bar{p}_t^{\text{dis}}\right) + E_{t-1}, h\left(-\tilde{d}_t + d_t - r_t^+ + r_t^-\right) + E_{t-1}\right\} \end{cases} \tag{A9}$$

Based on (11), (A3), (A8), and (A9), (9)-(15) can be rewritten as follows.

$$\underline{f}_t \le E_t \le \bar{f}_t \tag{A10}$$

If there is a feasible solution in (9)-(15), formulation (A10) should be non-empty. It implies that:

$$\underline{f}_t \le \bar{f}_t \tag{A11}$$

In detail, each term of $\underline{f}_t$ should be less than each term of $\bar{f}_t$ for any time period t. Consequently, we can obtain the three groups of inequalities.

$$\begin{cases} \underline{E}_t \le \bar{E}_t \\ h\left(\bar{p}_t^{\text{dis}}\right) \le h\left(-\bar{p}_t^{\text{ch}}\right) \\ h\left(-\tilde{d}_t + d_t - r_t^+ + r_t^-\right) \le h\left(-w_t - p_t^{\text{PV}} - \tilde{d}_t + d_t - r_t^+ + r_t^-\right) \end{cases} \tag{A12}$$

$$\begin{cases} -\tilde{d}_t + d_t - r_t^+ + r_t^- \ge -\bar{p}_t^{\text{ch}} \\ \bar{p}_t^{\text{dis}} \ge -w_t - p_t^{\text{PV}} - \tilde{d}_t + d_t - r_t^+ + r_t^- \end{cases} \tag{A13}$$

$$\begin{cases} E_{t-1} \le \min\left\{\bar{E}_t - h\left(-\tilde{d}_t + d_t - r_t^+ + r_t^-\right), \bar{E}_t - h\left(\bar{p}_t^{\text{dis}}\right)\right\} \\ E_{t-1} \ge \max\left\{\underline{E}_t - h\left(-w_t - p_t^{\text{PV}} - \tilde{d}_t + d_t - r_t^+ + r_t^-\right), \underline{E}_t - h\left(-\bar{p}_t^{\text{ch}}\right)\right\} \end{cases} \tag{A14}$$

Based on (A12)-(A14), some conclusions can be summarized.

1) Inequalities in (A12) are always satisfied according to (10), (11), and (14).

2) Inequalities in (A13) are independent of the state variable E_t and they should be always satisfied for any realizations of uncertainties. So (A13) can be regarded as a precondition and (A15) can be obtained for brevity.

$$\begin{cases} -\tilde{d}_t + \underline{d}_t - \bar{r}_t^+ + \underline{r}_t^- \ge -\bar{p}_t^{\text{ch}} \\ \bar{p}_t^{\text{dis}} \ge -\underline{w}_t - \underline{p}_t^{\text{PV}} - \tilde{d}_t + \bar{d}_t - \underline{r}_t^+ + \bar{r}_t^- \end{cases} \tag{A15}$$

Reorganize (A15) and thus (21) is proved.

3) Inequalities in (A14) are associated with the regions of E_{t-1}. Note that it is a sufficient condition to ensure that there is a feasible solution in E_t.

Inequalities in (A14) should be satisfied for any realization of uncertainty. There will be:

$$\begin{cases} E_{t-1} \le \min\left\{\bar{E}_t - h\left(-\tilde{d}_t + \underline{d}_t - R_t^+\right), \bar{E}_t - h\left(\bar{p}_t^{\text{dis}}\right)\right\} \\ E_{t-1} \ge \max\left\{\underline{E}_t - h\left(-\underline{w}_t - \underline{p}_t^{\text{PV}} - \tilde{d}_t + \bar{d}_t + R_t^-\right), \underline{E}_t - h\left(-\bar{p}_t^{\text{ch}}\right)\right\} \end{cases} \tag{A16}$$

Note that inequalities in (A16) are only the conditions for E_{t-1} to guarantee the range of E_t nonempty. And E_{t-1} also needs to satisfy its physical constraint (11). Then, we can obtain:

$$\begin{cases} \bar{E}_{t-1}^{\text{true}} = \min\left\{\bar{E}_t - h\left(-\tilde{d}_t + \underline{d}_t - R_t^+\right), \bar{E}_t - h\left(\bar{p}_t^{\text{dis}}\right), \bar{E}_{t-1}\right\} \\ \underline{E}_{t-1}^{\text{true}} = \max\left\{\underline{E}_t - h\left(-\underline{w}_t - \underline{p}_t^{\text{PV}} - \tilde{d}_t + \bar{d}_t + R_t^-\right), \right. \\ \qquad \left. \underline{E}_t - h\left(-\bar{p}_t^{\text{ch}}\right), \underline{E}_{t-1}\right\} \end{cases} \tag{A17}$$

The equations in (A17) provide the feasible multi-stage robust regions of one time period. To ensure feasibility during all the scheduling periods, the equations in (A17) should be extended to the whole time periods.

Recursively, for $t = T$, it is clear that $\bar{E}_T^{\text{true}} = \bar{E}_T$ and $\underline{E}_T^{\text{true}} = \underline{E}_T$. For $t = T-1$, we have (A18) based on (A17).

$$\begin{cases} \bar{E}_{T-1}^{\text{true}} = \min\left\{\bar{E}_T^{\text{true}} - h\left(-\tilde{d}_T + \underline{d}_T - R_T^+\right), \bar{E}_T^{\text{true}} - h\left(\bar{p}_T^{\text{dis}}\right), \bar{E}_{T-1}\right\} \\ \underline{E}_{T-1}^{\text{true}} = \max\left\{\underline{E}_T^{\text{true}} - h\left(-\underline{w}_T - \underline{p}_T^{\text{PV}} - \tilde{d}_T + \bar{d}_T + R_T^-\right), \right. \\ \qquad \left. \underline{E}_T^{\text{true}} - h\left(-\bar{p}_T^{\text{ch}}\right), \underline{E}_{T-1}\right\} \end{cases} \tag{A18}$$

For $t = T-2$, it holds that:

$$\begin{cases} \bar{E}_{T-2}^{\text{true}} = \min\Big\{ \bar{E}_{T-1}^{\text{true}} - h\left(-\tilde{d}_{T-1} + \underline{d}_{T-1} - R_{T-1}^{+}\right), \\ \qquad \bar{E}_{T-1}^{\text{true}} - h\left(\bar{p}_{T-1}^{\text{dis}}\right), \bar{E}_{T-2} \Big\} \\ \underline{E}_{T-2}^{\text{true}} = \max\Big\{ \underline{E}_{T-1}^{\text{true}} - h\left(-\underline{w}_{T-1} - \underline{p}_{T-1}^{\text{PV}} - \tilde{d}_{T-1} + \bar{d}_{T-1} + R_{T-1}^{-}\right), \\ \qquad \underline{E}_{T-1}^{\text{true}} - h\left(-\bar{p}_{T-1}^{\text{ch}}\right), \underline{E}_{T-2} \Big\} \end{cases} \tag{A19}$$

By recursion, (22) is satisfied for any time period t.
Q.E.D.

REFERENCES

[1] S. Li, C. Ye, Y. Ding *et al*., "Reliability assessment of renewable power systems considering thermally-induced incidents of large-scale battery energy storage," *IEEE Transactions on Power Systems*, vol. 38, no. 4, pp. 3924-3938, Jul. 2023.

[2] A. Akrami, M. Doostizadeh, and F. Aminifar, "Power system flexibility: an overview of emergence to evolution," *Journal of Modern Power Systems and Clean Energy*, vol. 7, no. 5, pp. 987-1007, Sept. 2019.

[3] S. Mei, Q. Tan, Y. Liu *et al*., "Optimal bidding strategy for virtual power plant participating in combined electricity and ancillary services market considering dynamic demand response price and integrated consumption satisfaction," *Energy*, vol. 284, p. 128592, Dec. 2023.

[4] X. Chen, Y. Yang, J. Song *et al*., "Hybrid energy storage system optimization with battery charging and swapping coordination," *IEEE Transactions on Automation Science and Engineering*, doi: 10.1109/TASE.2023.3292189

[5] Y. Chen and W. Wei, "Robust generation dispatch with strategic renewable power curtailment and decision-dependent uncertainty," *IEEE Transactions on Power Systems*, vol. 38, no. 5, pp. 4640-4654, Sept. 2023.

[6] S. K. Panda and B. Subudhi, "A review on robust and adaptive control schemes for microgrid," *Journal of Modern Power Systems and Clean Energy*, vol. 11, no. 4, pp. 1027-1040, Jul. 2023.

[7] B. Chen, J. Wang, X. Lu *et al*., "Networked microgrids for grid resilience, robustness, and efficiency: a review," *IEEE Transactions on Smart Grid*, vol. 12, no. 1, pp. 18-32, Jan. 2021.

[8] J. Lai, X. Lu, X. Yu *et al*., "Stochastic distributed secondary control for AC microgrids via event-triggered communication," *IEEE Transactions on Smart Grid*, vol. 11, no. 4, pp. 2746-2759, Jul. 2020.

[9] A. Bharatee, P. K. Ray, and A. Ghosh, "A power management scheme for grid-connected PV integrated with hybrid energy storage system," *Journal of Modern Power Systems and Clean Energy*, vol. 10, no. 4, pp. 954-963, Jul. 2022.

[10] M. M. Baggu, A. Nagarajan, D. Cutler *et al*., "Coordinated optimization of multiservice dispatch for energy storage systems with degradation model for utility applications," *IEEE Transactions on Sustainable Energy*, vol. 10, no. 2, pp. 886-894, Apr. 2019.

[11] R. Sioshansi, P. Denholm, J. Arteaga *et al*., "Energy-storage modeling: state-of-the-art and future research directions," *IEEE Transactions on Power Systems*, vol. 37, no. 2, pp. 860-875, Mar. 2022.

[12] S. M. Hosseini, R. Carli, and M. Dotoli, "Robust optimal energy management of a residential microgrid under uncertainties on demand and renewable power generation," *IEEE Transactions on Automation Science and Engineering*, vol. 18, no. 2, pp. 618-637, Apr. 2021.

[13] L. Luo, S. S. Abdulkareemet, A. Rezvani *et al*., "Optimal scheduling of a renewable-based microgrid considering photovoltaic system and battery energy storage under uncertainty," *Journal of Energy Storage*, vol. 28, p. 101306, Feb. 2020.

[14] C. Huang, H. Zhang, Y. Song *et al*., "Demand response for industrial Micro-grid considering photovoltaic power uncertainty and battery operational cost," *IEEE Transactions on Smart Grid*, vol. 12, no. 4, pp. 3043-3055, Jul. 2021.

[15] Z. Xu, X. Guan, Q. Jia *et al*., "Performance analysis and comparison on energy storage devices for smart building energy management," *IEEE Transactions on Smart Grid*, vol. 3, no. 4, pp. 2136-2147, Dec. 2012.

[16] R. Aboli, M. Ramezani, and H. Falaghi, "Joint optimization of day-ahead and uncertain near real-time operation of microgrids," *International Journal of Electrical Power & Energy Systems*, vol. 107, pp. 34-46, May 2019.

[17] J. Zhu, S. Huang, Y. Liu *et al*.,"Optimal energy management for grid-connected microgrids via expected-scenario-oriented robust optimization," *Energy*, vol. 216, p. 119224, Feb. 2021.

[18] M. Wu, J. Xu, L. Zeng *et al*., "Two-stage robust optimization model for park integrated energy system based on dynamic programming," *Applied Energy*, vol. 308, p. 118249, Feb. 2022.

[19] A. Lorca and X. Sun, "Multistage robust unit commitment with dynamic uncertainty sets and energy storage," *IEEE Transactions on Power Systems*, vol. 32, no. 3, pp. 1678-1688, May 2017.

[20] M. Zhou, Q. Zhai, and Y. Zhou, "Economic dispatch of energy storage system in Micro-grid," *IOP Conference Series: Materials Science and Engineering*, vol. 563, no. 5, pp. 1-12, Jul. 2019.

[21] Z. Guo, W. Wei, L. Chen *et al*., "Distribution system operation with renewables and energy storage: a linear programming based multistage robust feasibility approach," *IEEE Transactions on Power Systems*, vol. 37, no. 1, pp. 738-749, Jan. 2022.

[22] Y. Zhou, Q. Zhai, Z. Xu *et al*., "Multi-stage adaptive stochastic-robust scheduling method with affine decision policies for hydrogen-based multi-energy microgrid," *IEEE Transactions on Smart Grid*, doi: 10.1109/TSG.2023.3340727

[23] W. Liu, D. Wang, B. Liu *et al*., "Design and evaluation of micro energy network considering P2G-based storage system using two-stage stochastic programming," *IET Renewable Power Generation*, vol. 14, no. 17, pp. 3346-3355, Dec. 2020.

[24] W. Wei, F. Liu, S. Mei *et al*., "Robust energy and reserve dispatch under variable renewable generation," *IEEE Transactions on Smart Grid*, vol. 6, no. 1, pp. 369-380, Jan. 2015.

[25] Z. Guo, W. Wei, M. Shahidehpour *et al*., "Optimisation methods for dispatch and control of energy storage with renewable integration," *IET Smart Grid*, vol. 5, no. 3, pp. 137-160, Jun. 2022.

[26] Y. Zhou, Q. Zhai, L. Wu *et al*., "A data-driven variable reduction approach for transmission-constrained unit commitment of large-scale systems," *Journal of Modern Power Systems and Clean Energy*, vol. 11, no. 1, pp. 254-266, Jan. 2023.

[27] Q. Zhai, Y. Zhou, X. Li *et al*., "Nonanticipativity and all-scenario-feasibility: the state of the art, challenges, and future in dealing with the uncertain load and renewable energy," *Proceedings of the CSEE*, vol. 40, no. 20, pp. 6418-6433, Sept. 2020.

[28] Á. Lorca, X. Sun, E. Litvinov *et al*., "Multistage adaptive robust optimization for the unit commitment problem," *Operations Research*, vol. 64, no. 1, pp. 32-51, Feb. 2016.

[29] Y. Zhou, Q. Zhai, and L. Wu, "Multistage transmission-constrained unit commitment with renewable energy and energy storage: implicit and explicit decision methods," *IEEE Transactions on Sustainable Energy*, vol. 12, no. 2, pp. 1032-1043, Apr. 2021.

[30] B. Xu, Y. Wang, Y. Dvorkin *et al*., "Scalable planning for energy storage in energy and reserve markets," *IEEE Transactions on Power Systems*, vol. 32, no. 6, pp. 4515-4527, Nov. 2017.

[31] N. G. Cobos, J. M. Arroyo, N. Alguacil *et al*., "Robust energy and reserve scheduling considering bulk energy storage units and wind uncertainty," *IEEE Transactions on Power Systems*, vol. 33, no. 5, pp. 5206-5216, Jan. 2018.

[32] Z. Tang, J. Liu, Y. Liu *et al*., "Stochastic reserve scheduling of energy storage system in energy and reserve markets," *International Journal of Electrical Power & Energy Systems*, vol. 123, p. 106279, Dec. 2020.

[33] Z. Tang, Y. Liu, L. Wu *et al*., "Reserve model of energy storage in day-ahead joint energy and reserve markets: a stochastic UC solution," *IEEE Transactions on Smart Grid*, vol. 12, no. 1, pp. 372-382, Jan. 2021.

[34] H. A. Bafrani, M. Sedighizadeh, M. Dowlatshahi *et al*., "Spinning reserve stochastic model of compressed air energy storage in day-ahead joint energy and reserve market using information gap decision theory method," *International Journal of Electrical Power & Energy Systems*, vol. 141, p. 108123, Oct. 2022..

[35] H. Akhavan-Hejazi and H. Mohsenian-Rad, "Optimal operation of independent storage systems in energy and reserve markets with high wind penetration," *IEEE Transactions on Smart Grid*, vol. 5, no. 2, pp. 1088-1097, Mar. 2014.

[36] M. Kazemi, H. Zareipour, N. Amjady *et al*., "Operation scheduling of battery storage systems in joint energy and ancillary services markets," *IEEE Transactions on Sustainable Energy*, vol. 8, no. 4, pp. 1726-1735, Oct. 2017.

[37] T. Song, K. Li, X. Han *et al*., "Coordinated operation strategy of energy storage system participating in multiple application scenarios," *Automation of Electric Power Systems*, vol. 45, no. 19, pp. 43-51, Oct. 2021.

[38] M. A. Ortega-Vazquez and D. S. Kirschen, "Estimating the spinning

reserve requirements in systems with significant wind power generation penetration," *IEEE Transactions on Power Systems*, vol. 24, no. 1, pp. 114-124, Feb. 2009.

[39] A. Zakariazadeh, S. Jadid, and P. Siano, "Smart microgrid energy and reserve scheduling with demand response using stochastic optimization," *International Journal of Electrical Power & Energy Systems*, vol. 63, pp. 523-533, Dec. 2014.

[40] R. Mafakheri, P. Sheikhahmadi, and S. Bahramara, "A two-level model for the participation of microgrids in energy and reserve markets using hybrid stochastic-IGDT approach," *International Journal of Electrical Power & Energy Systems*, vol. 119, p. 105977, Jul. 2020.

[41] P. Fazlalipour, M. Ehsan, and B. Mohammadi-Ivatloo, "Risk-aware stochastic bidding strategy of renewable micro-grids in day-ahead and real-time markets," *Energy*, vol. 171, pp. 689-700, Mar. 2019.

[42] X. Zhu, B. Zeng, H. Dong *et al*., "An interval-prediction based robust optimization approach for energy-hub operation scheduling considering flexible ramping products," *Energy*, vol. 194, p. 116821, Mar. 2020.

[43] Y. Su, F. Liu, Z. Wang *et al*., "Multi-stage robust dispatch considering demand response under decision-dependent uncertainty," *IEEE Transactions on Smart Grid*, vol. 14, no. 4, pp. 2786-2797, Jul. 2023.

[44] Y. Tang and Q. Zhai, "Minimum power transfer limit planning for grid-connected microgrid" in *Proceedings of 2022 IEEE PES General Meeting (PESGM)*, Denver, USA, Jul. 2022, pp. 1-6.

[45] Y. Tang, Q. Zhai, and J. Zhao, "Multi-stage robust economic dispatch with virtual energy storage and renewables based on a single level model," *IEEE Transactions on Automation Science and Engineering*, doi: 10.1109/TASE.2023.3312379

[46] H. Qiu, W. Gu, X. Xu *et al*., "A historical-correlation-driven robust optimization approach for microgrid dispatch," *IEEE Transactions on Smart Grid*, vol. 12, no. 2, pp. 1135-1148, Apr. 2021.

Ye Tang received the B.S. degree in automation and the M.S. degree in control theory and control engineering from Chang'an University, Xi'an, China, in 2016 and 2019. She is currently pursuing the Ph.D. degree in control science and engineering, Xi'an Jiaotong University. Her research interests include multi-stage robust optimization, planning and scheduling of microgrid systems with renewable energy resources, and energy storage systems.

Qiaozhu Zhai received the B.S. and M.S. degrees in applied mathematics and the Ph.D. degree in systems engineering from Xi'an Jiaotong University, Xi'an, China, in 1993, 1996, and 2005, respectively. He is currently a Professor at the Systems Engineering Institute of Xi'an Jiaotong University. His research interests include optimization of large-scale systems and integrated resource bidding and scheduling in electricity market.

Yuzhou Zhou received the B.S. degree in automation and the Ph.D. degree in control science and engineering from Xi'an Jiaotong University, Xi'an, China, in 2015 and 2021, respectively. From 2019 to 2020, he was a Visiting Scholar with the Stevens Institute of Technology, Hoboken, USA. He is currently an Assistant Professor with the Systems Engineering Institute of Xi'an Jiaotong University. His research interests include planning and scheduling of energy system with renewable energy resources and energy storage systems.